





A new alternative route for achieving energy saving in intensified reactive-extractive distillation system with a surprise discovery

Zong Yang Kong^a , Eduardo Sánchez-Ramírez^b, Ao Yang^c, Yong Li^c, Juan Gabriel Segovia-Hernández^{b,*}, Basil T. Wong^c, Jaka Sunarso^{d,*} 

^a School of Engineering and Technology, Sunway University, No. 5, Jalan Universiti, Bandar Sunway, 47500 Selangor Darul Ehsan, Malaysia

^b Universidad de Guanajuato, Campus Guanajuato, División de Ciencias Naturales y Exactas, Departamento de Ingeniería Química, Noria Alta s/n, 36050 Guanajuato, Gto, Mexico

^c College of Safety Engineering, Chongqing University of Science & Technology, Chongqing 401331, PR China

^d Research Centre for Sustainable Technologies, Faculty of Engineering, Computing and Science, Swinburne University of Technology, Jalan Simpang Tiga, 93350 Kuching, Sarawak, Malaysia

ARTICLE INFO

Keywords:

Process intensification
Reactive-extractive distillation
Separation
Ternary azeotropic mixture
Resource conservation

ABSTRACT

In contrast to other intensified distillation processes, it has been well-reported that the intensified reactive-extractive distillation (RED) cannot provide any energy savings with respect to its non-intensified counterpart. Motivated by this limitation, this study aims to explore other alternative intensified configurations to improve RED system performance. Specifically, we investigate the combined use of thermally-coupled and side-stream as a hybrid process intensification (PI) technique to enhance energy efficiency, as most existing studies have applied these techniques individually without examining their potential synergy. We begin by selecting a ternary azeotropic mixture that has been previously studied using both RED and intensified thermally-coupled RED (T-DCRED). Using these configurations as base case, we further investigate 2 other alternative hybrid side-stream thermally-coupled RED (ST-DCRED) configurations to evaluate their energy savings potential. During our investigation, we unexpectedly discovered that the T-DCRED could achieve 12 % energy savings compared to the conventional RED, which contradicts with previous studies. Additionally, our study into 2 newly proposed ST-DCRED configurations also showed potential energy savings of up to 13 % compared to conventional RED. These results suggest that hybrid ST-DCRED offer a promising alternative to traditional PI methods, such as thermally-coupled or dividing-wall configurations, for improving energy efficiency in RED systems.

1. Introduction

The hybrid reactive-extractive distillation (RED) system has gained widespread use for separating ternary azeotropic mixtures. It has the benefits of combining both reaction and azeotropic separation within a single column, as opposed to performing these operations sequentially in 2 separate unit operations, analogous to the reactive distillation (RD) process. The additional feature in the RED is that it typically requires additional injection of an external solvent to facilitate the separation of the azeotropic mixtures. As a result, RED is often considered an example of process intensification (PI), as it tends to reduce the number of unit operations needed for a given azeotropic mixture separation. For example, the separation of the ternary azeotropic mixture of tetrahydrofuran, ethanol, and water has been extensively studied, with over 10

research papers published to date [1–4]. Traditionally, this separation was carried out using a three-column extractive distillation process. However, studies have demonstrated that RED can reduce the number of columns from 3 to 2, reflecting its potential as a PI technique [5]. Additionally, RED can also offer significant energy savings compared to conventional extractive distillation methods.

To further promote energy savings, recent research has even explored adding an additional layer of PI to the RED system, aiming to reduce the number of columns from 2 to just 1, even though RED is already being considered as a PI unit. The motivation of this is derived from numerous studies in conventional distillation (or even advanced distillation systems like extractive distillation), which have shown that applying PI can lead to significant energy savings. This benefit is mainly due to the ability of intensified processes to eliminate/minimize the

* Corresponding authors.

E-mail addresses: gsegovia@ugto.mx (J.G. Segovia-Hernández), jsunarso@swinburne.edu.my (J. Sunarso).

<https://doi.org/10.1016/j.cej.2024.158498>

Received 17 October 2024; Received in revised form 18 November 2024; Accepted 9 December 2024

Available online 12 December 2024

1385-8947/© 2024 The Author(s). Published by Elsevier B.V. This is an open access article under the CC BY license (<http://creativecommons.org/licenses/by/4.0/>).

remixing effect typically seen in non-intensified distillation systems. Consequently, recent efforts aim to leverage PI in the RED system to make it even more energy-efficient and appealing. For example, Liu et al. [6] explored the separation of ethyl acetate, ethanol, and water using both the double column RED (DCRED) and the dividing wall RED (DWRED) configurations. They found that while DWRED offered a cost reduction of around 8 % compared to DCRED, it surprisingly exhibited approximately 3 % higher energy consumption. This result is unusual since PI techniques (e.g., dividing-wall or thermally-coupled) generally lead to energy savings in other types of distillation systems [7–9]. The reason for the higher energy usage in DWRED compared to DCRED in this case, however, was not clearly detailed by Liu et al. [6]. In our opinion, this could be reasonable given that the PI application (i.e., DWRED) already yields some cost savings. However, we still find this observation surprising, as it differs from the typical outcomes reported in conventional distillation systems. Without closely examining both flowsheets, this higher energy consumption in DWRED might go unnoticed. Similarly, Yang et al. [10] reported a slightly higher energy usage for DWRED relative to DCRED, even though DWRED achieved lower costs and reduced CO₂ emission. Notably, several other studies on intensified DCRED systems have also struggled to demonstrate energy savings when compared to their non-intensified counterparts. In fact, to the best of our knowledge, most studies on intensified DCRED have not shown energy savings when compared to the DCRED base case [6,10–14].

A recently proposed alternative to further enhance energy savings in the RED system involves a simple switch in the sequence of the RED column (REDC) and the solvent regeneration column (SRC) [15]. This adjustment, when further intensified through thermal coupling, resulted in an impressive 21 and 28 % reduction in cost and energy consumption, respectively, compared to the non-intensified configuration. Apart from the column switching method [15], our literature review reveals that there are no other studies in the existing body of research have successfully demonstrated energy savings in intensified RED systems. As a result, we are motivated to further explore on whether there are any other alternative configurations, beyond those suggested in the work of Chen et al. [15], that could help to enhance the performance of the RED system. Other than thermally-coupled or dividing wall configuration, our literature review has indicated that the “side-stream” is another PI technique that is frequently applied in both conventional and advanced distillation processes [16,17]. The benefits of having multiple side-streams have also been explored in literature [18]. However, no studies have yet examined the combined benefits of thermally-coupled systems and side-stream configurations as a single hybrid PI technique for improving energy efficiency in RED systems [19,20]. To the best of our knowledge, most existing studies have only applied these techniques individually without exploring the potential synergy of combining them.

Following this, we aim to evaluate the advantages of integrating both thermally-coupled and side-stream as a single hybrid PI technique to enhance energy savings in the RED system. To start with, we will select a ternary azeotropic mixture previously studied for separation using both RED and intensified RED (i.e., a thermally-coupled RED (T-DCRED)). Using these configurations as a benchmark, we will then examine the alternative hybrid side-stream thermally-coupled RED (ST-DCRED) to assess its potential drawbacks and benefits in comparison to the configurations reported in previous work. During our investigation, we “unexpectedly” discover that the intensified T-DCRED system could achieve significant energy savings compared to the conventional DCRED base case. This finding was unexpected, as previous studies have consistently shown that intensified T-DCRED does not provide any energy savings over the conventional base case. Thus, while our primary focus is on exploring the new hybrid ST-DCRED configurations, here we also seek to analyze why the intensified T-DCRED simulated in our study demonstrates energy savings, contrary to earlier findings. The remainder of the manuscript is organized as follows: Section 2 outlines the methodology used, detailing the conventional and intensified RED,

along with the design and optimization procedures. Section 3 provides an in-depth discussion of the findings, and Section 4 concludes the work with a summary of the study.

2. Methodology

Fig. 1 graphically illustrates the flow of this study. In general, a suitable RED process was first chosen as the base case, and its simulation was reproduced in this work. Next, 3 intensified configurations were simulated, i.e., a T-DCRED and 2 new hybrid ST-DCRED configurations. All 4 configurations were optimized to enable a fair comparison, and the results were evaluated based on total reboiler energy consumption and total annual cost (TAC).

2.1. Description of base case

The base case for this study is taken from the work of Zhang et al. [5], which involves a feed stream of 100 kmol h⁻¹ containing 30 mol% acetonitrile (ACN), 30 mol% isopropanol (IPA), and 40 mol% water. This process was selected because it is one of the earliest examples demonstrating the use of DCRED, and its corresponding intensified processes have been further explored in subsequent studies [21]. The first column in this process is commonly referred to as the REDC, which receives the fresh feed along with externally injected ethylene oxide (EO), typically introduced below the fresh feed location. The EO flow-rate is generally determined by the water content in the fresh feed, as EO and water react in a 1:1 stoichiometric ratio (Eq. (1)), to produce ethylene glycol (EG). Additionally, extra EG solvent is injected at the top of the REDC to enhance azeotropic separation, as the *in situ* produced EG may not always suffice for the effective azeotropic separation. Note that the hydration reaction of EO occurring in the REDC is uncatalyzed and is therefore expected to take place throughout the entire column [5]. The ACN is recovered at the REDC distillate, while the remaining mixture containing IPA and EG is routed to the SRC. In the SRC, IPA is recovered at the distillate, and EG is collected as the bottom product. The regenerated EG is cooled before being recirculated back to the REDC. Any excess solvent in the system is removed through a purging mechanism.



$$r_1 \left(\frac{mol}{scm^3} \right) = 3.15 \times 10^9 \exp \left(\frac{-9547}{T} \right) x_{water} x_{EO} \quad (1)$$

Here, the original process from Zhang et al. [5] was first reproduced in Aspen Plus V14. The same Nonrandom Two-Liquid (NRTL) fluid package was used as in the work of Zhang et al. [5], and the corresponding binary interaction parameters are provided in Table S1. Note that the reliability and suitability of using the NRTL model for the ACN/IPA/Water system in the RED process have been validated by previous studies and therefore, it is not repeated again in this work. As for the reproduced process, we observed only minor differences in most streams and column parameters from the results, which once again confirms the accuracy and reliability of the reproduced model. We then proceeded to optimize the reproduced base case, with the details of the optimization algorithm provided in Section 2.3 for the sake of better manuscript flow. Fig. 2 illustrates the optimized base case for the separation of the ACN/IPA/water mixture, while the optimization outcomes are illustrated in Fig. S1. The TAC stabilized at around \$0.95 million. In Fig. 2, the REDC configuration consumes approximately 147 kW and utilizes low-pressure steam (LPS), whereas the SRC configuration requires significantly more reboiler energy of about 1087 kW, which is roughly 10 times that of REDC, and uses high-pressure steam (HPS). This results in a total reboiler duty of approximately 1234 kW. As for the total number of stages, the REDC contains 69 stages while the SRC contains 11 stages.

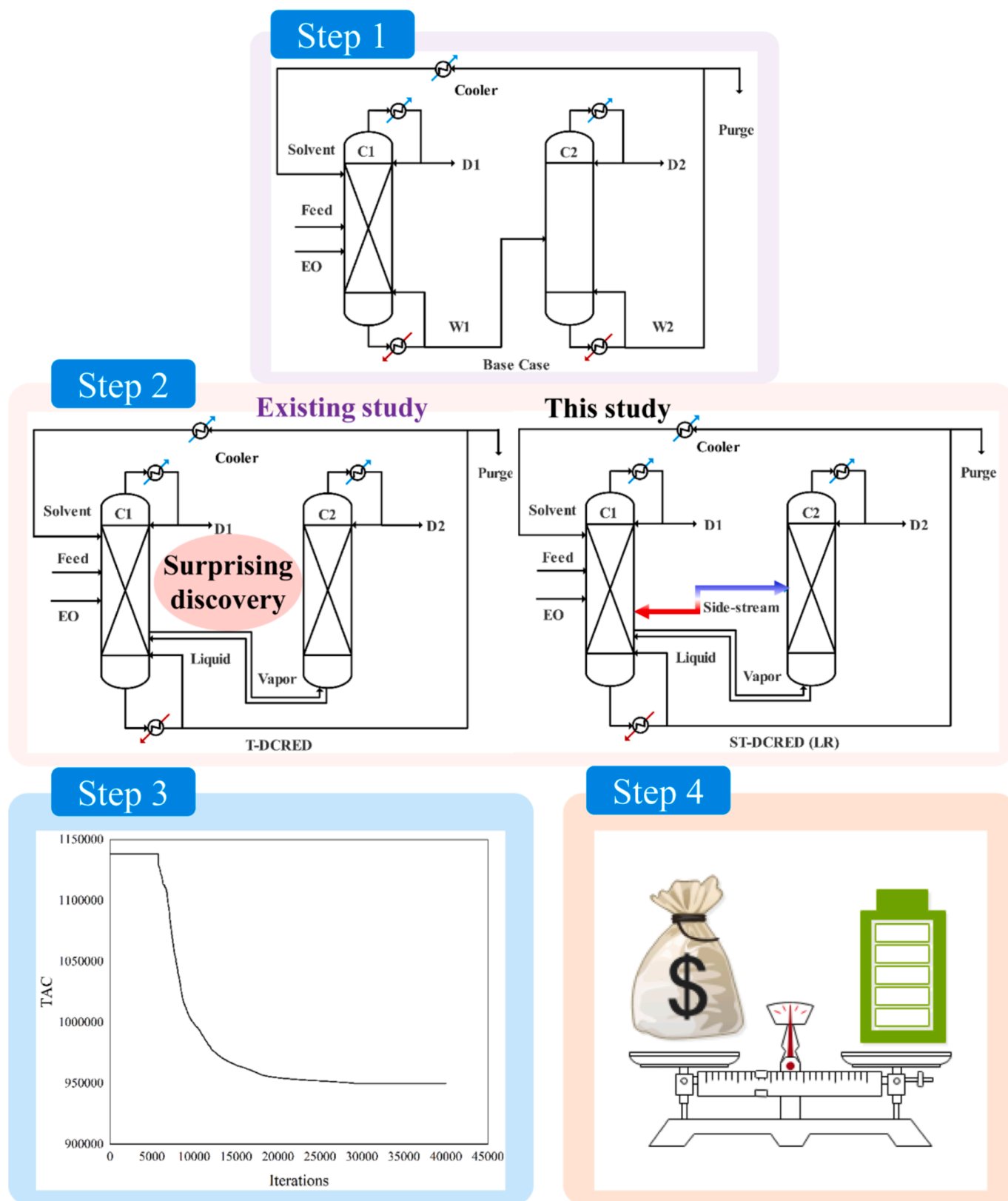


Fig. 1. Graphical summary of this study.

2.2. Description of intensified configurations

In this work, three intensified configurations are investigated (Fig. 3), all of which are derived from the optimized base case (Fig. 2). The first configuration is a T-DCRED, which has already been explored

by previous study [21]. We include this configuration to provide a benchmark for comparing our two newly proposed intensified configurations because the T-DCRED has been shown in numerous studies to exhibit contradictory behavior by failing to demonstrate energy savings compared to its non-intensified counterpart [11,12,21]. The second and

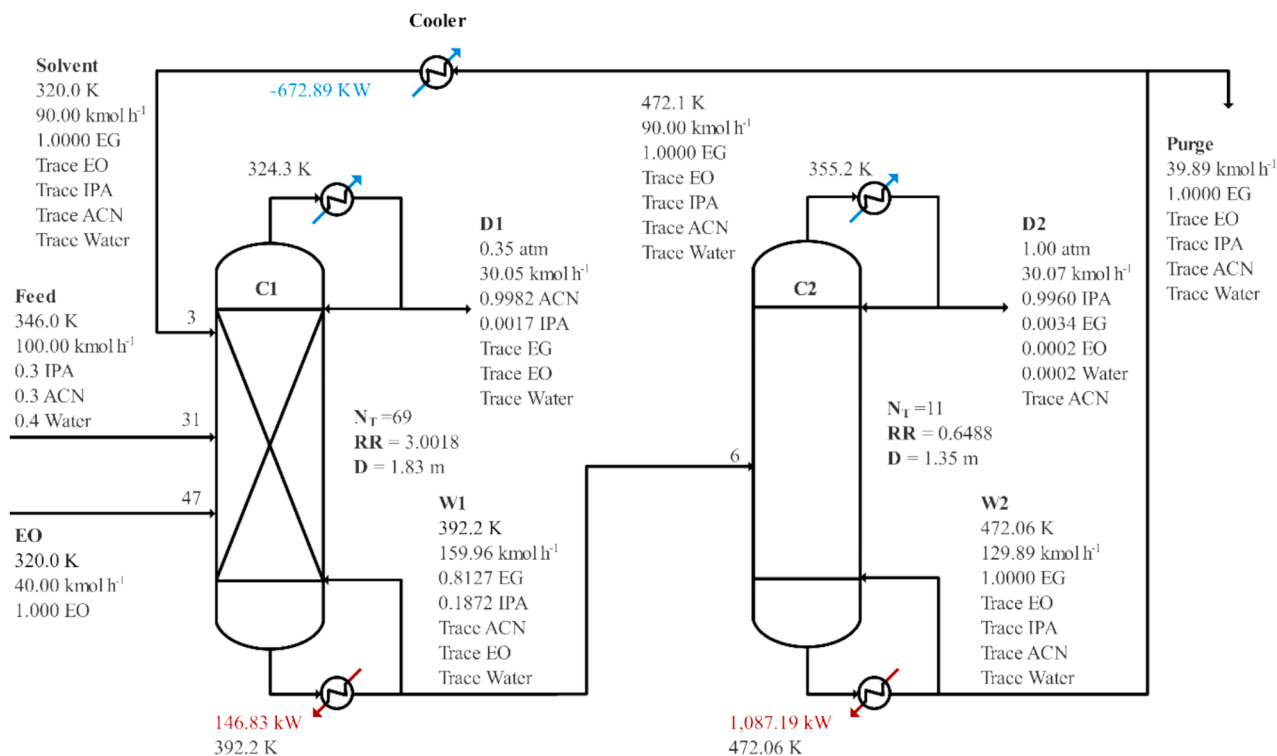


Fig. 2. Optimized DCREd for the separation of ACN/IPA/water (Base case).

third configurations are entirely new and, to our knowledge, have not been explored in the existing literature. This section provides a brief overview of these intensified processes, while their results and comparisons are discussed in detail in Section 3.

2.2.1. Conventional T-DCRED

In this configuration, thermal coupling between the two original columns is achieved by removing the reboiler at the bottom of the SRC and directly transferring the bottom liquid to the REDC. To ensure vapor flow back to the SRC, a vapor side draw is introduced at the same stage of the REDC and returned to the SRC. Due to the liquid-vapor interconnection link between the two columns, some water and EO are diverted to the SRC before the complete reaction described in Eq. (1) can occur, significantly impacting distillate product's purity. To mitigate this issue, it is necessary to incorporate a reaction zone within the SRC. This approach is reasonable since the EO hydration reaction (Eq. (1)) is uncatalyzed, making it difficult to control where the reaction happens [5]. As both water and EO are directed into the SRC due to the interconnection link, they can react within the SRC itself. As a result, the reactions occur throughout both columns (Fig. 3(b)), rather than being restricted to the REDC alone. To our knowledge, there are generally two methods described in the literature for designing a T-DCRED configuration. The first method involves maintaining the same total number of stages as in the optimized base case. This approach enables a fair comparison of energy savings under consistent stage counts, meaning that any reductions in TAC can be attributed primarily to energy savings rather than changes in capital cost. This method has been employed in some existing studies [9,22,23]. Another more common approach is to optimize the intensified configuration [6,24,25] and then compare its performance with the optimized base case. It is crucial to ensure that the same optimization algorithm is used for both configurations so that any observed benefits are due to the nature of the configuration itself, rather than the differences in the optimization method. Nevertheless, it is worth noting that previous studies on intensified RED systems have shown that, even after optimization, while the TAC of the intensified case may be lower than that of the base case, this does not necessarily

imply that its energy consumption is also reduced [6,11,12,14,25]. Such an observation contradicts findings reported for other types of distillation systems (e.g., ideal, extractive, or reactive distillation). In this work, the latter (i.e., second) approach is utilized where we also optimized the T-DCRED and compared the performance against the optimized base case.

2.2.2. New hybrid ST-DCRED

Fig. 3(c) and (d) shows the conceptual design of the two new hybrid ST-DCRED configurations, referred to as ST-DCRED (LR) (Fig. 3(c)) and ST-DCRED (RL) (Fig. 3(d)). These configurations aim to enhance DCRED performance by integrating two PI strategies, i.e., thermally-coupled and side stream, in a hybrid approach. Structurally, both configurations follow the T-DCRED framework shown in Fig. 3(b), where thermal-coupling of the two original columns is achieved by eliminating the reboiler at the bottom of the SRC and directly transferring the bottom liquid to the REDC. A vapor side draw is also present at the same stage of the REDC to ensure vapor flow back to the SRC. The reaction zone in both hybrid ST-DCRED configurations is analogous to that of the T-DCRED, with reactions occurring throughout both columns. The key difference between the ST-DCRED configurations and the T-DCRED lies in the addition of a liquid side-stream between the REDC and SRC. In ST-DCRED (LR), the liquid side-stream diverts a portion of the flow from the REDC to the SRC (i.e., from left to right), while in ST-DCRED (RL), it channels some flow from the SRC to the REDC (i.e., from right to left). At this stage, the optimal location for the side draw and side-stream feed stage, as well as the side-stream flowrate, are not yet determined. We believe it would be beneficial to include these variables in the optimization process. Consequently, both ST-DCRED configurations are optimized to compare their performance against the optimized T-DCRED and base case (i.e., DCRED).

2.3. Optimization procedure

In all the case studies, the main objective is to reduce the TAC, which is closely linked to the heat duty, the utility requirements, and the size of

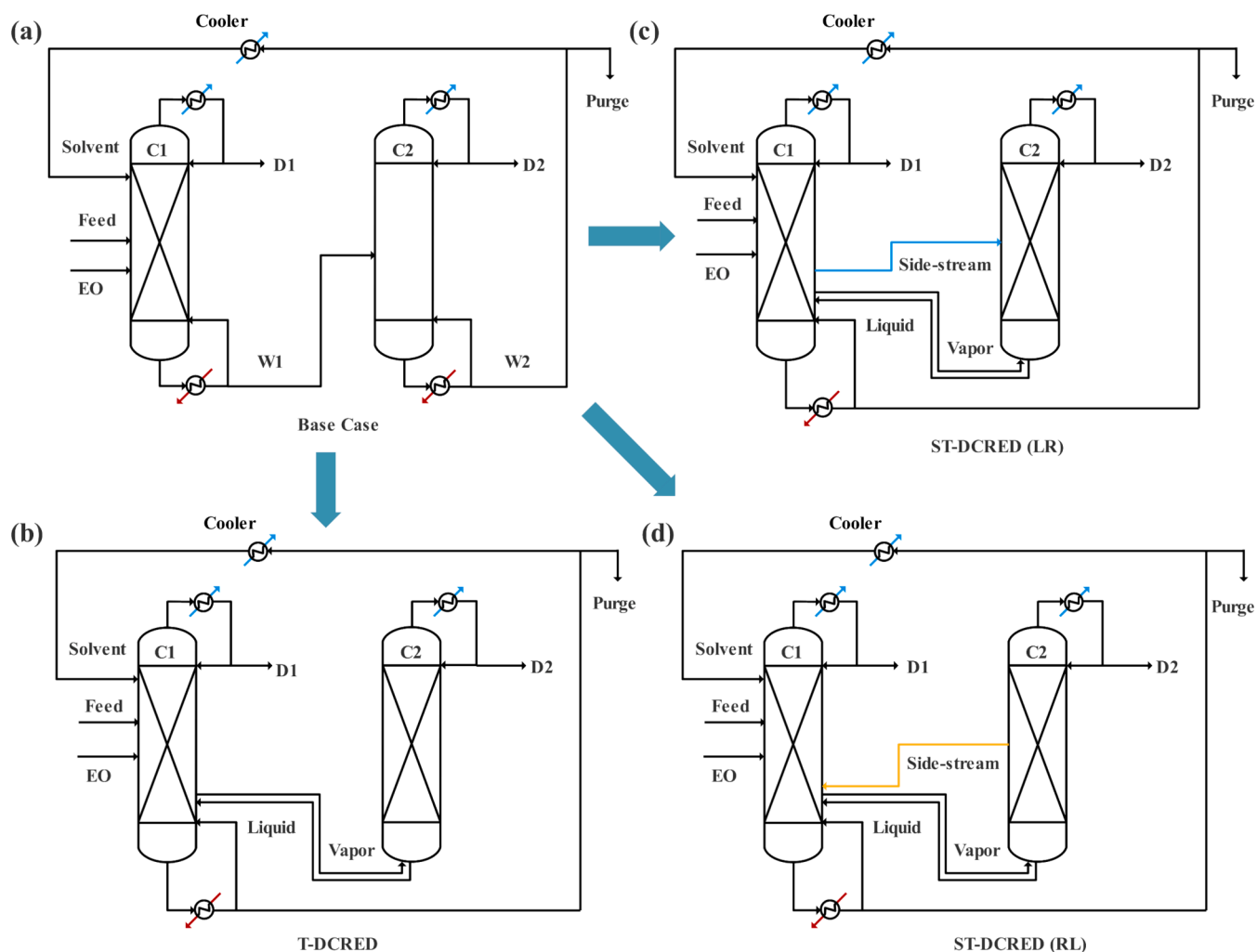


Fig. 3. Overview of three intensified configurations investigated in this work, derived from the (a) DCRED base case: (b) the T-DCRED, (c) the ST-DCRED (LR), and (d) the ST-DCRED (RL).

the column. Reaching this goal depends on achieving the required recoveries and purities in each product stream, which can be mathematically represented by Eq. (2). The TAC is calculated according to Eq. (3) where C_{TM} represents the total cost of the i -module, C_{ut} is the cost of j -utility, t_{ri} is the payback period. Additional information to these cost estimation can be found in Eqs. (S1)–(S4) in the [Supporting Information](#).

$$\min(\text{TAC}) = f(\mathbf{N}_{tn}, \mathbf{N}_{fn}, \mathbf{R}_m, \mathbf{F}_m, \mathbf{D}_{cn}, \mathbf{H}_{un}, \mathbf{S}_{dl}, \mathbf{F}_{sd}, \mathbf{S}_{ff} \dots)$$

$$\text{subject to } \vec{y}_m \geq \vec{x}_m \quad (2)$$

$$\text{TAC}(\$/y) = \frac{\sum_{i=1}^n C_{TMi}}{t_{ri}} + \sum_{j=1}^m C_{uj} \quad (3)$$

The optimization process generally involves multiple parameters. These can include \mathbf{N}_m for the total number of column stages, \mathbf{N}_{fn} for feed stages, \mathbf{R}_m for the reflux ratio, \mathbf{F}_m representing distillate fluxes, \mathbf{D}_{cn} for column diameter, \mathbf{H}_{un} as hold up, \mathbf{S}_{dl} for side-draw location, \mathbf{F}_{sd} for feed stage of side-draw, and \mathbf{S}_{ff} for side-draw flowrate, and \mathbf{y}_m and \mathbf{x}_m as vectors for the obtained and required products purities, respectively. Note that the \mathbf{D}_{cn} is included as an optimization variable in order to ensure feasible designs by avoiding impractical column sizes, such as excessively small or unreasonably large diameters that may occur when relying solely on default values from Aspen Plus. Also, it is important to highlight that in different configurations, the optimization variables may have particular variables that other schemes may not have and

altogether, there are about 15–20 continuous and discrete variables for each process configuration. It is important to consider that, since product stream flows are influenced by chemical reactions, the purities of key components in these streams must be treated as constraints in the optimization problem. The design and optimization of process configuration present complex, nonlinear, and multivariable challenges, involving both continuous and discrete variables. Additionally, the objective functions used for optimization can be nonconvex, possibly leading to local optima while respecting certain constraints. The constraints associated with each case study are initially the same for all. For example, minimum purity constraints of 99.8 mol.%, 99.6 mol.%, and 99.92 mol.% were considered for ACN, IPA, and EG, respectively.

In each case, some particular physical constraints were considered. For example, for the case of T-DCRED, as there is a vapor stream between REDC and SRC, the stream was fed into the N stage of the SRC. In this same case study, the vapor split from the REDC to the SRC, and the return from the liquid split to the REDC, were considered to be in the same stage of the REDC. For the ST-DCRED (LR), there were some similar physical design constraints where two streams from the REDC to the SRC were considered; a vapor split and a liquid split. Both streams were fed into different N stage of the SRC, but not necessarily out of the same stage of the REDC. As in the case of T-DCRED, the liquid split exiting the SRC is fed onto the REDC at the stage where the vapor split left. For the ST-DCRED (RL), there are other specific restrictions. There is only one vapor split that originates from the REDC to the SRC, which is

fed onto the SRC at stage N. On the other hand, there are two liquid splits from the SRC to the REDC, one of these liquid streams enters the REDC at the same stage where a vapor stream exits.

To handle the complexities of optimizing process routes, we used a stochastic method called Differential Evolution with Tabu List (DETL). Based on Darwin's natural selection, DE is similar to Genetic Algorithms (GA) but encodes decision variables as floating-point numbers instead of bit strings. Srinivas and Rangaiah [26] showed that adding tabu search to DE enhances performance by preventing revisits to previously explored regions, reducing unnecessary function evaluations. The hybrid DETL approach combines DE steps with a tabu list to track evaluated points and avoid duplicates. A maximum number of generations serve as the convergence criterion. The optimization was implemented using a hybrid platform combining Microsoft Excel and Aspen Plus, communicating through Dynamic Data Exchange (DDE) and COM technology. COM, a Windows-based system, enables interprocess communication and supports software integration. Excel assigns values to process variables, which are simulated in Aspen Plus. The results are returned to Excel for analysis, and new variable values are proposed by the optimization algorithm. During optimization, the algorithm assigns vectors to design variables but must account for physical constraints. For instance, if it proposes a total stage count (X) and feed stage (Y), Y must be less than X. Since the algorithm does not inherently recognize these relationships, constraints must be built into the code to ensure the proposed values make physical sense and impact the objective function directly. This process allows the algorithm to generate valid new vectors for evaluation.

To express internal constraints in the optimization algorithm, especially when one design variable depends on another, the relationship can be mathematically described. Let the vector of decision variables be x , including design parameters. The algorithm aims to minimize or maximize an objective function $f(x)$, with internal constraints forming equations between variables. For instance, if variable x_i influences x_j , this is expressed via Eq. (4).

$$x_j = g(x_i) \quad (4)$$

In Eq. (4), x_i is determined by the algorithm, and x_j depends on x_i . The algorithm iteratively assigns values to these variables until the constraint is satisfied. This process continues until convergence is achieved, ensuring that the internal constraints, such as the relationship between stages and feed positions in a column, are respected. By embedding these internal constraints in the optimization code, variables can be redefined based on previously proposed values, directly impacting the objective function. This approach addresses issues like "variable overlap" and ensures the design aligns with real-world conditions, as seen in the assignment of values for feed stages and reactive columns [24]. In addition, the internal constraints help to avoid infeasible configurations resulting from variable crossover, which can have significant physical implications. For example, to prevent scenarios where the number of reaction stages exceeds the total number of stages, internal checks were programmed to immediately verify and compare related variables. This ensured that the optimization process remained consistent with physical feasibility, thereby improving overall optimization accuracy and avoiding impractical designs.

In this study, the specific process routes were optimized using the following parameters for the DETL method: 200 individuals, 300 generations, a tabu list consisting of 50 % of the individuals, a tabu radius of 0.0000025, and crossover and mutation rates of 0.80 and 0.6, respectively. These settings were determined through a tuning process that involved preliminary testing, where various combinations of individuals and generations were evaluated to find the optimal parameters for achieving the best convergence performance with DETL.

3. Results and discussion

3.1. T-DCRED (A surprising case)

Fig. 4 displays the optimized flowsheet of the T-DCRED, with the corresponding optimization results shown in Fig. S2. The TAC stabilized at around \$0.879934 million. Such TAC reflects a 7 % reduction compared to the optimized DCRED base case presented in Section 2.2.1. Upon comparing Fig. 4 to Fig. 2, a notable reduction in total energy consumption of approximately 12.4 % is observed, decreasing from 1234 kW to 1080 kW. This result is unexpected as it appears to contradict previous findings reported in studies on intensified RED [6,11,12,14,25], which did not observe any energy savings. We will further explore and clarify this surprising outcome later, for the sake of maintaining a better manuscript flow. Here, it is important to recall that the T-DCRED now operates with only 1 reboiler due to the removal of the reboiler in the SRC. Consequently, the total reboiler duty of the T-DCRED corresponds solely to that of the REDC. From a capital cost point of view, there is an immediate decrease in the cost associated with the eliminated reboiler, as well as the cost of servicing the reboiler. However, as a result of eliminating this reboiler, operational aspects can also be observed in the scheme, for example, a slight increase in the reflux ratio of the second column, as well as a slight increase in the thermal load of the first column. Also, the heating utility required for the REDC reboiler now necessitates HPS instead of LPS due to the high boiling point of the regenerated EG at the REDC bottom. Recall that in the optimized base case (Fig. 2), the REDC reboiler only utilized LPS, which has a unit cost that is 21 % lower than HPS. Other than that, the total number of stages has also changed, with the REDC requiring 1 additional stage and the SRC require 2 less stages, resulting in an overall reduction of 1 stage compared to the optimized base case (Fig. 2). As for the column diameter, there was a noticeable trade-off between the 2 columns, i. e., the diameter of the REDC increased by 9.3 %, from 1.83 m to 2 m, while the SRC diameter decreased by 33.3 %, from 1.35 m to 0.9 m. We believe this trade-off has a marginal impact on the overall TAC. The reduction in the total number of stages reduces the total capital cost, while the lower reboiler duty leads to reduced total operating costs. These collective reduction leads to a lower TAC as compared to the optimized DCRED.

We compare next the results obtained for the T-DCRED configuration with an existing study reported by Teh et al. [21], who also examined intensified DCRED configurations for the separation of the ACN/IPA/water mixture. In their study, Teh et al. [21] simulated both the T-DCRED and the DWRED, finding that the reboiler duty increased by 0.43 % and 2.15 %, respectively, compared to the conventional DCRED. The configuration reported by Teh et al. [21] may be argued to arise from the absence of process optimization. However, we believe that this might not be the sole reason, as many studies have already shown that intensified DCRED configurations do not necessarily result in energy savings even after optimization [6,11,12,14,25]. This makes the 12.4 % reduction in energy consumption achieved by our T-DCRED configuration particularly surprising. One reason Teh et al. [21] attributed for the lack of energy savings in T-DCRED configurations is the insufficient elimination of the remixing effect in intensified DCRED configurations, as determined from their analysis of the composition profile. To better understand this phenomenon, we also analyzed the composition profiles of the T-DCRED and DCRED in our study to identify any similar trends. The composition profiles for the first column of the T-DCRED and DCRED configurations are shown in Fig. 5. Note that although there are 5 different components in the REDC system (i.e., ACN, IPA, water, EO, and EG), we only focus on IPA and EG here since these are the components that flow into the SRC column and are most likely to exhibit remixing effects. From Fig. 5, it can be seen that the DCRED configuration shows a pronounced remixing effect, as indicated by the solid blue line. This remixing causes a peak in the purity of IPA, which is the desired product, followed by a decline as it nears the bottom of the

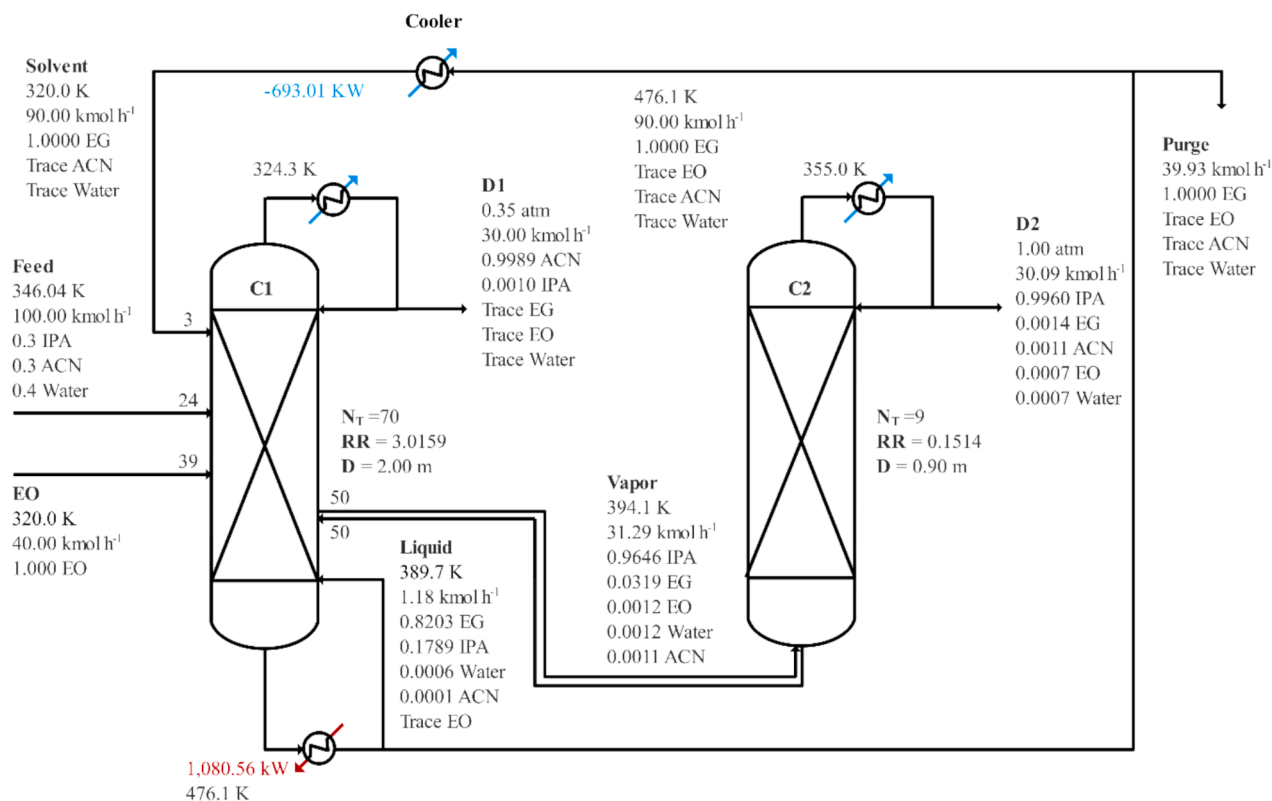


Fig. 4. The optimized flowsheet of T-DCRED.

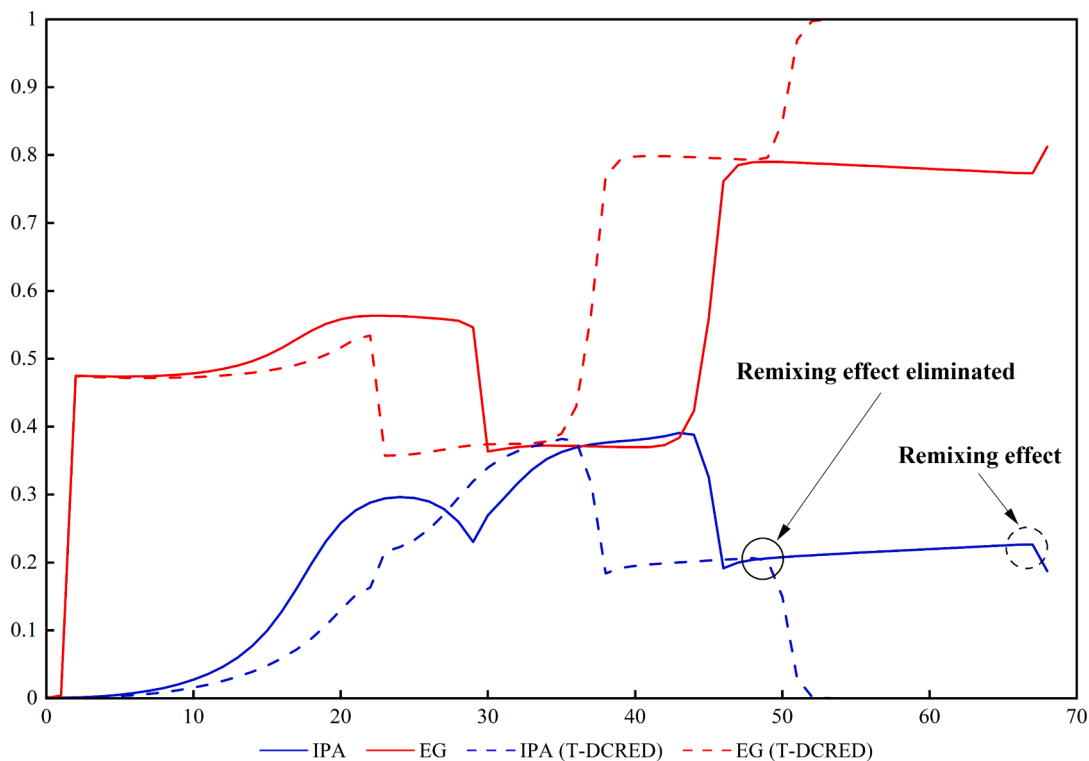


Fig. 5. Composition profile of the optimized DCRED base case and optimized T-DCRED.

column. Consequently, a lower quantity (and thus lower purity) of IPA is transferred to the SRC for further separation. A common strategy to mitigate this remixing effect and improve energy efficiency is to use a T-DCRED configuration. As shown in Fig. 5, the T-DCRED in this work

successfully eliminates the remixing effect, with the IPA withdrawn at its maximum purity (i.e., Stage 50). Upon comparing our composition profile with that of Teh et al. [21], we observed a similar trend in the extent to which the remixing effect was eliminated, with no significant

differences between the two studies. The only observable difference lies in the maximum IPA purity location where Teh et al. [21] reported the highest purity at the bottom of the REDC while in our case, the IPA composition decreases to zero as it reaches the bottom of REDC. The most plausible explanation to this is that Teh et al. [21] simulated the T-DCRED by eliminating the reboiler in the REDC, whereas in our simulation, we removed the reboiler in the SRC. As a result, the IPA withdrawal locations differs. Nevertheless, the IPA withdrawal location in both studies are at its maximum purity, unlike the DCRED where IPA is withdrawn at a lower purity. Therefore, we believe the energy savings observed in our work, which was missing in the work of Teh et al. [21], are not solely due to the composition profile.

Other than remixing effect and composition profile, another critical factor influencing the energy consumption of T-DCRED and DCRED is the internal vapor flowrate. An increase in the internal vapor flowrate within a distillation column generally leads to higher energy usage [27]. As a result, vapor flowrate serves as a useful metric for assessing the efficiency of different distillation systems. In our previous work aimed at understanding why some advanced intensified distillation configurations failed to deliver energy savings [28], we found that increased internal vapor flowrates were directly associated with higher heat energy consumption, which aligns with the findings of the work of Mo et al. [29]. This effect is particularly noticeable when a reboiler is involved, as elevated vapor flowrates often drive up the energy demands of the column. Table 1 presents a comparison of the average internal vapor flowrates for both the T-DCRED and DCRED configurations. For the DCRED, the internal vapor flowrates of the REDC and SRC were determined by calculating the average internal flowrate of the columns. In the case of T-DCRED, the SRC vapor flowrate was similarly calculated as the average internal column flowrate. However, the REDC in the T-DCRED exhibited two types of internal vapor flowrates: (1) the average flowrate for all stages above the side-draw location and (2) the average flowrate for all stages below the side-draw location.

From Table 1, we observe that the average internal vapor flowrate below the side-draw location in the REDC of the T-DCRED configuration is lower than the flowrate above the side-draw location. This contradicts the findings of Kong et al. [28] and Teh et al. [21], which suggest that the average internal vapor flowrate below the side-draw location in T-DCRED should be higher than that above the side-draw in order for energy savings to be realized. Their reasoning is that, above the side-draw, most of the vapor should divert to the column without the reboiler via the side-draw. However, this does not seem to be the case in our study. Furthermore, Kong et al. [28] indicated that when the average internal vapor flowrate below the side-draw location of the column with the reboiler surpasses that of the column without the reboiler, the intensified configuration may not achieve energy savings due to increased energy consumption associated with the higher vapor flowrate in the column with the reboiler. In our case, the vapor flowrate below the side-draw location of the REDC (which has the reboiler) in T-DCRED is indeed much higher than that of the SRC (which lacks the reboiler). Nonetheless, we still managed to achieve energy savings, which is quite unexpected and contradicts existing studies that follow this heuristic [15,28,30], where no energy savings were observed.

Until here, we have so far observed contradicting trends in the results of our T-DCRED compared to those reported by Teh et al. [21] and other

existing studies [15,28,30]. However, we now finally identify an observation that aligns with the findings of Teh et al. [21] and other existing studies [15,28,30]. By “align”, we do not mean that we obtained identical results, but rather that our findings are consistent with the observations (or heuristic) highlighted by Teh et al. [21] and others [15,28,30]. Specifically, in the work of Teh et al. [21], they pointed out that the higher energy consumption in intensified processes can be attributed to the lower feed inlet temperature of the SRC (which also corresponds to the temperature at the bottom of the REDC). They demonstrated that the REDC bottom temperature in the T-DCRED configuration was lower than in the DCRED, resulting in additional energy required to raise the low inlet temperature to the operating temperature of the SRC. In our case, the bottom temperature of the REDC in T-DCRED (Fig. 4) appears to be slightly higher at 394 K, than that of the DCRED at 392 K (Fig. 2). This could be one of the reasons why our T-DCRED achieves energy savings compared to the DCRED.

Besides comparing the result trends with those observed by Teh et al. [21], we also identified an additional observation that may be of interest and worth discussing, which has not been revealed in previous studies. Upon examining Fig. 4 alongside Fig. 2, we noticed that the composition of the liquid bottom stream returning from the SRC to the REDC in Fig. 4 is quite similar to the composition of the liquid bottom stream from the REDC to the SRC in Fig. 2. In Fig. 4, the liquid bottom stream consists of approximately 82 mol.% EG and 18 mol.% IPA, while in Fig. 2, a similar composition is observed, with around 82 mol.% EG and 18 mol.% IPA. While we cannot precisely state whether this similarity contributes to the energy savings achieved by our T-DCRED system compared to previous studies, it is a notable phenomenon that has not been commonly observed in existing studies on intensified DCRED systems. For instance, the aforementioned streams in both the T-DCRED and DCRED systems in the work of Teh et al. [21] show different compositions, and similar variations were observed in other intensified DCRED studies that reported lower energy savings [6,11,12,14,25]. Hence, we speculate that this could be one reason why our T-DCRED is able to provide significant energy savings compared to the DCRED.

3.2. New hybrid ST-DCREDS

Fig. 6 presents the optimized flowsheets for the two newly proposed ST-DCRED configurations, with the corresponding optimization results provided in Fig. S3. In Fig. 6(a), the additional liquid side-stream diverts a portion of the flow from the REDC to the SRC (i.e., left to right), hence we designate it as ST-DCRED (LR). Conversely, in Fig. 6(b), the liquid side-stream directs the flow from the SRC to the REDC (i.e., right to left), leading to the designation of ST-DCRED (RL). For ST-DCRED (LR), the TAC stabilized at around \$0.879934 million and for ST-DCRED (RL), it stabilized at approximately \$0.877 million. Compared to the optimized DCRED base case (Fig. 2), both ST-DCRED configurations achieve a similar TAC reduction to that of the T-DCRED, with both the ST-DCRED providing a slightly greater reduction. In terms of energy consumption, both ST-DCRED configurations demonstrate significant energy savings of up to 13 % compared to the optimized DCRED base case, which is comparable to the energy savings achieved by the T-DCRED.

In terms of column configuration, the ST-DCRED (LR) (Fig. 6(a)) requires approximately 5 fewer stages in the REDC and 2 fewer stages in the SRC compared to the DCRED (Fig. 2). Additionally, the diameters of both the REDC and SRC decrease by about 1.6 % and 31.9 %, respectively, relative to the DCRED. These reductions significantly lower the total capital cost of the proposed process. The combined benefits of reduced energy consumption, which lowered operational costs, and decreased capital investment due to fewer stages and smaller diameters, make the ST-DCRED (LR) superior to the DCRED. In fact, the ST-DCRED (LR) achieves the lowest TAC among the four configurations studied (i.e., DCRED, T-DCRED, ST-DCRED (LR), and ST-DCRED (RL)). The only trade-off in the ST-DCRED (LR) is similar to that of the T-DCRED where the hot utility consumed by the sole reboiler requires HPS instead of LPS,

Table 1
The column internal flowrate comparison of DCRED and T-DCRED.

Column	Average flowrate based on	DCRED (kmol h ⁻¹)	T-DCRED (kmol h ⁻¹)
1st	Whole column	71.54	n/a
	Above side-draw location	n/a	84.70
	Below side-draw location	n/a	65.38
2nd	Whole column	50.50	28.64
Total reboiler duty (kW)		1234	1081

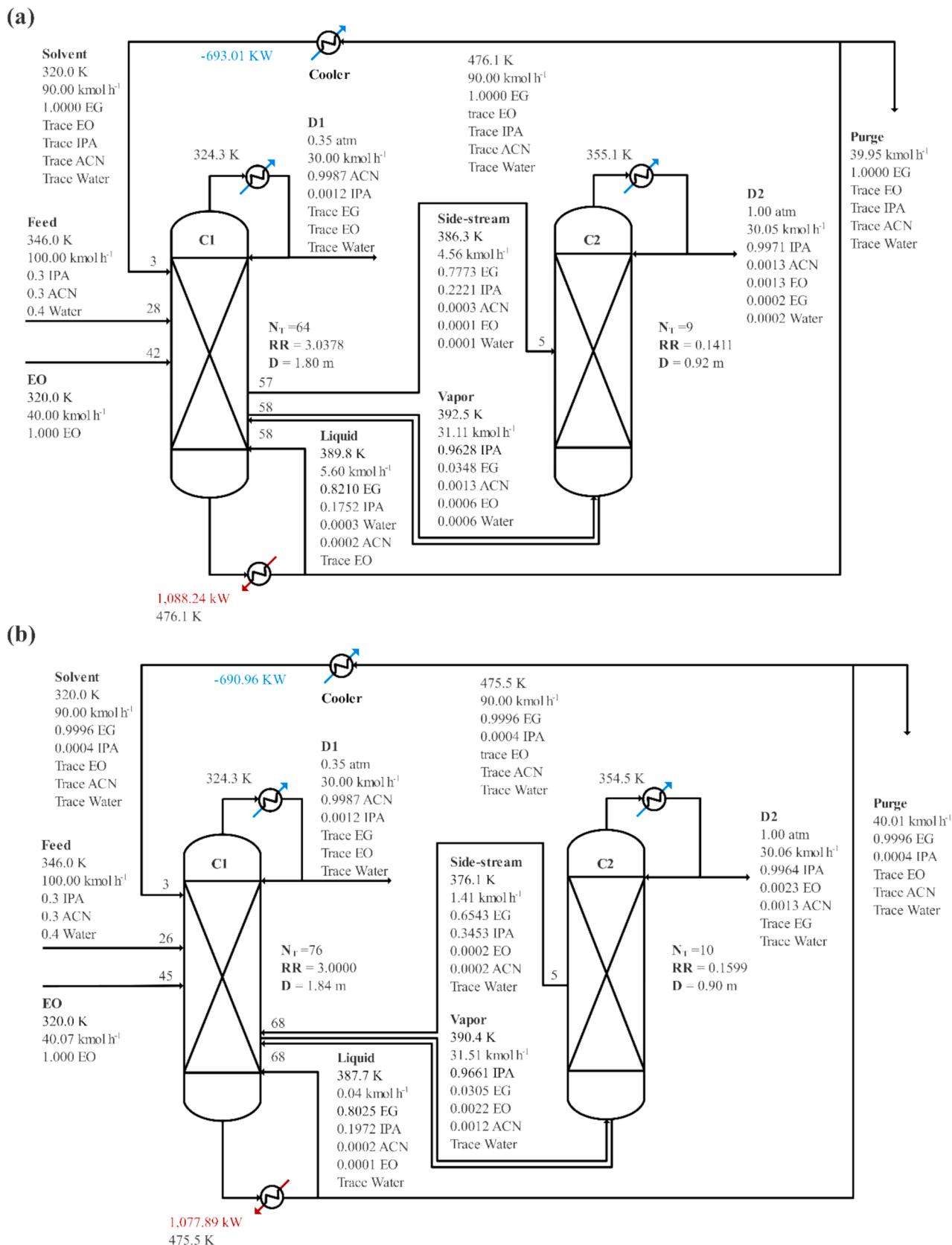


Fig. 6. The optimized flowsheet of (a) ST-DCRED (LR) and (b) ST-DCRED (RL).

as in the DCRED. Since HPS has a unit cost 21 % higher than LPS, this introduces a slight trade-off in operational cost savings. Nonetheless, this trade-off is outweighed by the overall reduction in reboiler duty and total capital cost. For the ST-DCRED (RL) (Fig. 6(b)), the total number of stages also changes, with the REDC requiring 7 additional stages and the SRC requiring 1 fewer stage, resulting in an overall increase of 6 stages compared to the optimized base case (Fig. 2). Regarding column diameter, the REDC sees a minimal increase of less than 1 %, while the diameter of SRC decreases significantly by 33.3 %, from 1.35 m to 0.9 m. Consequently, it is expected that the total capital cost for the ST-DCRED (RL) would be slightly higher than that of the DCRED. In addition to the increased capital cost, the ST-DCRED (RL) also requires a higher grade of hot utility (i.e., HPS) compared to the DCRED. As explained earlier, HPS has a significantly higher unit cost than LPS and therefore, this partially offsets the operational cost savings. However, our results suggest that the increase in capital cost and the use of more expensive hot utility are still outweighed by the overall reduction in reboiler duty. However, the cost advantage of the ST-DCRED (RL) is not as significant as that of the ST-DCRED (LR), resulting in a slightly higher TAC for the ST-DCRED (RL) compared to the ST-DCRED (LR). Nonetheless, the ST-DCRED (RL) still demonstrates a lower TAC than the T-DCRED and, more notably, a much lower TAC than the DCRED.

Analogous to the analysis conducted for the T-DCRED, we aim to evaluate the composition profile, the internal vapor flowrate, the feed inlet temperature to SRC, and the composition of the liquid bottom stream returning from the SRC to the REDC, as was performed for the T-DCRED. Fig. 7 presents the composition profile for the REDC in both ST-DCRED configurations, with the composition profile of the T-DCRED also included for comparison. We will focus on IPA and EG, as these are the components that flow into the SRC and exhibited remixing effects. As

shown in Fig. 7, both ST-DCRED configurations successfully eliminate the remixing effect, similar to the T-DCRED. Therefore, we can conclude that not only does the T-DCRED, as discussed in Section 3.1, significantly reduce the remixing effect, thereby lowering the total reboiler duty, but the ST-DCRED configurations, which was never before reported in the literature also achieve this while offering comparable energy and cost performance relative to the T-DCRED.

In addition to their similarity in eliminating the remixing effect, there are notable differences between the two ST-DCRED configurations and the T-DCRED. In the ST-DCRED (LR), there are 2 withdrawal locations in the REDC, whereas the T-DCRED has only 1. The first withdrawal location in the ST-DCRED (LR) is similar to that in the T-DCRED, drawing IPA at its peak purity near the bottom of the column. However, the ST-DCRED (LR) also features an additional withdrawal location not present in the T-DCRED. As shown in Fig. 6(a), this additional side-draw is located on stage 57, where 4.56 kmol h^{-1} of liquid is transferred from the REDC to the SRC. This location and flowrate were determined through process optimization. Since the additional side-draw contains both EG and IPA as majority of its component and is transferred in liquid form rather than vapor, we speculate that some of the IPA will need to be redirected back to the REDC, where the reboiler will need to provide the necessary heat to vaporize it. This would cause the IPA to become mostly vapor and return again to the SRC via the thermal-coupled link, before finally exiting as the desired product through the distillate of the SRC. If our speculation holds, the IPA would take a longer pathway (i.e., a longer cycle), which may explain why the energy consumption of the ST-DCRED (LR) is higher compared to the ST-DCRED (RL) and T-DCRED. However, it is still lower than that of the base DCRED. In contrast, the ST-DCRED (RL) has only 1 withdrawal location in the REDC, similar to the T-DCRED, because the additional side-draw in this case transfers

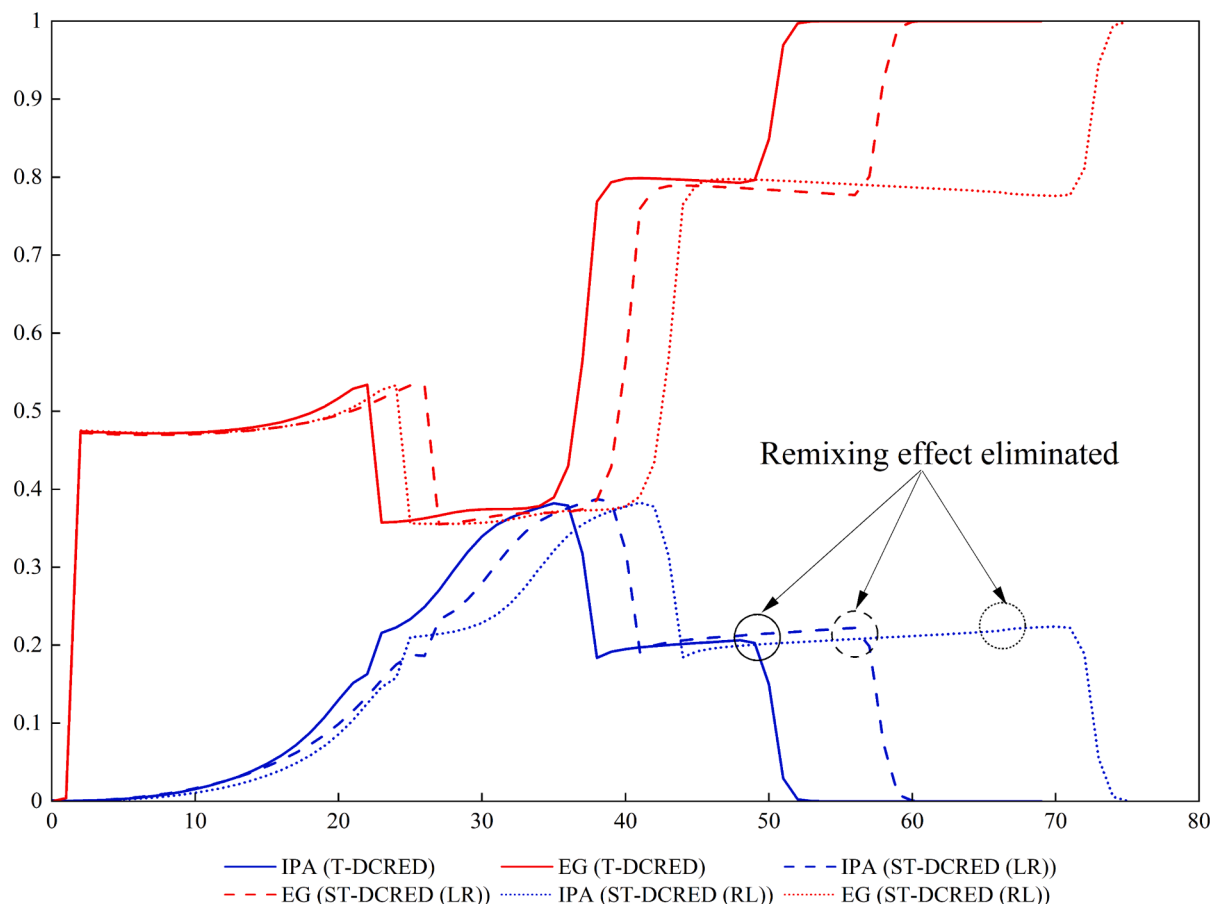


Fig. 7. Composition profile of the optimized T-DCRED, ST-DCRED (LR), and ST-DCRED (RL).

liquid from the SRC to the REDC (i.e., right to left). This side-draw is located on stage 5 of the SRC, transferring 1.41 kmol h^{-1} of liquid containing EG and IPA to the REDC, as shown in Fig. 6(b). The flowrate and location were also determined through optimization. Although the components in the additional side-draw are similar in both ST-DCRED configurations, it is important to highlight a key difference in how EG exits the process. Supposedly, the only way for EG to exit the process is through the bottom of the REDC. In the ST-DCRED (LR), the additional side-draw transfers a portion of EG to the SRC, and this portion must be redirected back to the REDC through the interconnection at the bottom of the SRC, creating a longer pathway. However, in the ST-DCRED (RL), EG from SRC is transferred via 2 different streams to the REDC. The first stream is through the interconnection stream as in the case of ST-DCRED (LR) and T-DCRED while the second stream is the additional side-draw that is only present in the ST-DCRED (RL). Hence, this additional side-draw in the ST-DCRED(RL) facilitates a more efficient exit for EG from the process. This avoids the need for EG to be transferred back and forth between the REDC and SRC, which shortens the overall route. Additionally, the side-draw flowrate in the ST-DCRED (RL) is much smaller compared to the ST-DCRED (LR). As a result, it is expected that the ST-DCRED (RL) will consume slightly less reboiler energy than the ST-DCRED (LR) and T-DCRED, although the difference may not be substantial, which could be a relevant clue to consider them thermodynamically equivalent. Nonetheless, we must clarify that this is purely our speculation, aimed at explaining why the ST-DCRED (RL) delivers the best performance among the three configurations (in terms of energy consumption) and why the ST-DCRED (LR) may not outperform the T-DCRED.

Table 2 provides a comparison of the average internal vapor flowrates for both ST-DCRED configurations, with the T-DCRED also included for comparison. Similar trends are observed as in the T-DCRED, where the average internal vapor flowrate below the side-draw in the REDC is lower than the flowrate above it. Additionally, in the T-DCRED, the vapor flowrate below the side-draw in the REDC (which contains the reboiler) is significantly higher than that in the SRC (which lacks a reboiler). These findings contradict previous studies (Teh et al. [21] and others [15,28,30]), which suggest that for energy savings to occur, the internal vapor flowrate below the side-draw should be higher than that above and the fact that when the internal vapor flowrate below the side-draw in the column with the reboiler exceeds that of the column without the reboiler, energy savings are unlikely, as the increased vapor flowrate in the reboiler column leads to higher energy consumption. Despite these contradictions, our study has still achieved energy savings, which is both unexpected and in opposition to the conclusions of previous research that follow this heuristic [6,11,12,14,25].

Regarding the feed temperature entering the SRC, the bottom temperatures of the REDC in both ST-DCRED (LR) and ST-DCRED (RL) configurations (Fig. 6) are approximately 392 K and 390 K, respectively. As mentioned in Section 3.1, previous studies have demonstrated that a higher feed inlet temperatures to the SRC in intensified processes can lead to lower energy consumption compared to the conventional base case. In the ST-DCRED (LR) configuration, although the feed

temperature to the SRC is similar to that of the optimized DCRED base case, we did not achieve a better energy savings. We believe this is due to the presence of an additional side-draw from the REDC to the SRC. The temperature of this side-draw (i.e., around 386 K) is lower than the feed inlet temperature into the SRC in the DCRED base case, which likely explains why the energy consumption of the ST-DCRED (LR) is slightly higher than the base case. In the case of the ST-DCRED (RL), the feed temperature to the SRC is also slightly lower than in the DCRED base case, suggesting that energy consumption should be higher. However, this is not the case, as Fig. 6(b) shows that the ST-DCRED (RL) actually has the lowest total reboiler energy consumption. We believe this is because reboiler energy consumption is influenced not just by the feed inlet temperature but also by other factors, such as internal vapor flowrates and interconnection flowrates, as discussed earlier.

Finally, regarding the composition of the liquid bottom stream returning from the SRC to the REDC, we observed that the composition of this stream in both ST-DCRED configurations (Fig. 6) is nearly identical to that of the T-DCRED configuration (Fig. 4), with only a slight difference of around 2 mol.% in the case of ST-DCRED (RL) (Fig. 6(b)). Given that the composition of the liquid bottom stream returning from the SRC to the REDC in the intensified configurations is quite similar to that of the liquid bottom stream in the DCRED base case (Fig. 2), this similarity may have contributed to the marginal energy savings observed in both ST-DCRED configurations, similar to the savings seen in the T-DCRED.

4. Conclusion

In conclusion, this study explores alternative configurations to improve the energy efficiency of the RED process since it has been widely reported that the intensified RED cannot provide any energy savings as compared to other intensified distillation processes. Using a ternary azeotropic mixture that has been well-studied in both conventional and intensified RED processes as a benchmark, we examined the performances of 2 new hybrid ST-DCRED configurations based on TAC and energy consumption. Surprisingly, our findings revealed that the intensified T-DCRED can provide significant energy savings up to 12 % compared to the conventional DCRED system, which contradicts previous studies that reported no energy savings from intensified DCRED. We analyzed this unexpected result using several heuristics from earlier studies, including its potential elimination of remixing effects, internal vapor flowrate, and inlet temperatures to the SRC. However, our findings suggest that the trends observed here do not fully align with prior studies. Instead, a new phenomenon was observed, i.e., the composition of the liquid bottom stream returning from the SRC to the REDC closely resembled the flow behavior of the conventional RED system, potentially explaining the observed energy savings. Regarding the two proposed ST-DCRED configurations, our simulations demonstrated their potential to achieve up to 13 % energy savings compared to the DCRED. This improvement is similarly attributed to the mimicking of flow behavior between the SRC and REDC, which may contribute to enhanced energy efficiency. Therefore, we conclude that these hybrid configurations present a promising alternative to traditional intensification techniques, such as thermally-coupled or dividing-wall configurations, for realizing energy savings in RED systems.

One potential limitation, in our view, is that the original RED system is already a complex, intensified process combining both reaction and azeotropic separation in a single unit. Adding thermal coupling would further complicate the operation, potentially degrading the control performance of the system. Therefore, combining the thermal coupling with a side-stream as a hybrid PI approach to improve energy efficiency may impact the controllability of the system significantly. Future work should therefore address how to balance the energy savings achieved through PI, along with the control deterioration associated with it. Another limitation to consider is that the RED process uses a highly flammable reactant (i.e., EO). This study focuses on enhancing energy

Table 2

The column internal flowrate comparison between the two proposed ST-DCRED configurations and T-DCRED.

Column	Average flowrate based on	T-DCRED (kmol h ⁻¹)	ST-DCRED (LR) (kmol h ⁻¹)	ST-DCRED (RL) (kmol h ⁻¹)
1st	Whole column	n/a	n/a	n/a
	Above side-draw location	84.70	81.67	72.48
	Below side-draw location	65.38	57.95	42.62
2nd	Whole column	28.64	28.42	29.51
	Total reboiler duty (kW)	1080	1088	1078

efficiency but does not address the safety concerns related to the hazardous nature of EO. As such, future work can explore the use of a safer, more environmentally friendly reactant in combination with the proposed process to improve both energy efficiency and safety. Lastly, our opinion is that it seems like we have found an intensified RED (i.e., T-DCRED) that exhibits a different trend in the result compared to previous studies, but it is only for a specific mixture (i.e., ACN/IPA/Water). Thus, it may be premature to generalize the findings at this stage, and further studies are needed to validate the results presented here. One potential approach is to extend the application of the proposed configurations to the separation of other ternary azeotropic mixtures.

CRedit authorship contribution statement

Zong Yang Kong: Writing – review & editing, Writing – original draft, Visualization, Validation, Supervision, Software, Resources, Project administration, Methodology, Investigation, Formal analysis, Data curation, Conceptualization. **Eduardo Sánchez-Ramírez:** Writing – review & editing, Writing – original draft, Visualization, Validation, Software, Methodology, Investigation, Formal analysis, Data curation. **Ao Yang:** Writing – review & editing, Writing – original draft, Visualization, Validation, Supervision, Software, Resources, Project administration, Methodology, Investigation, Formal analysis, Data curation, Conceptualization. **Yong Li:** Visualization, Software, Resources, Formal analysis. **Juan Gabriel Segovia-Hernández:** Writing – review & editing, Visualization, Supervision, Software, Resources, Project administration, Methodology. **Basil T. Wong:** Writing – review & editing. **Jaka Sunarso:** Writing – review & editing, Supervision, Software, Resources, Project administration, Funding acquisition, Conceptualization.

Declaration of competing interest

The authors declare that they have no known competing financial interests or personal relationships that could have appeared to influence the work reported in this paper.

Acknowledgments

Z.Y. Kong gratefully acknowledged the support from Sunway University Malaysia.

Appendix A. Supplementary data

Supplementary data to this article can be found online at <https://doi.org/10.1016/j.cej.2024.158498>.

Data availability

Data will be made available on request.

References

- [1] Y. Zhao, T. Zhao, H. Jia, X. Li, Z. Zhu, Y. Wang, Optimization of the composition of mixed entrainer for economic extractive distillation process in view of the separation of tetrahydrofuran/ethanol/water ternary azeotrope, *J. Chem. Technol. Biotechnol.* 92 (2017) 2433–2444, <https://doi.org/10.1002/jctb.5254>.
- [2] C. Wang, Y. Zhuang, Y. Qin, Y. Dong, L. Liu, L. Zhang, J. Du, Design and eco-efficiency analysis of sustainable extractive distillation process combining preconcentration and solvent recovery functions for separating the tetrahydrofuran/ethanol/water ternary multi-azeotropic mixture, *Process Saf. Environ. Prot.* 159 (2022) 795–808, <https://doi.org/10.1016/j.psep.2022.01.060>.
- [3] Y. Zhao, K. Ma, W. Bai, D. Du, Z. Zhu, Y. Wang, J. Gao, Energy-saving thermally coupled ternary extractive distillation process by combining with mixed entrainer for separating ternary mixture containing bioethanol, *Energy* 148 (2018) 296–308, <https://doi.org/10.1016/j.energy.2018.01.161>.
- [4] Y. Zhao, H. Jia, X. Geng, G. Wen, Z. Zhu, Y. Wang, Comparison of conventional extractive distillation and heat integrated extractive distillation for separating tetrahydrofuran/ethanol/water, *Chem. Eng. Trans.* 61 (2017) 751–756, <https://doi.org/10.3303/CET1761123>.
- [5] Y.R. Zhang, T.W. Wu, I.L. Chien, Intensified hybrid reactive-extractive distillation process for the separation of water-containing ternary mixtures, *Sep. Purif. Technol.* 279 (2021), <https://doi.org/10.1016/j.seppur.2021.119712>.
- [6] J. Liu, J. Yan, W. Liu, J. Kong, Y. Wu, X. Li, L. Sun, Design and multi-objective optimization of reactive-extractive dividing wall column with organic Rankine cycles considering safety, *Sep. Purif. Technol.* 287 (2022) 120512, <https://doi.org/10.1016/j.seppur.2022.120512>.
- [7] A.A. Kiss, D.-J.-P.-C. Suszwalak, Innovative dimethyl ether synthesis in a reactive dividing-wall column, *Comput. Chem. Eng.* 38 (2012) 74–81, <https://doi.org/10.1016/j.compchemeng.2011.11.012>.
- [8] L. Shi, S.-J. Wang, K. Huang, D.-S.-H. Wong, Y. Yuan, H. Chen, L. Zhang, S. Wang, Intensifying reactive dividing-wall distillation processes via vapor recompression heat pump, *J. Taiwan Inst. Chem. Eng.* 78 (2017) 8–19, <https://doi.org/10.1016/j.jtice.2017.05.013>.
- [9] Y.C. Wu, P.H.C. Hsu, I.L. Chien, Critical assessment of the energy-saving potential of an extractive dividing-wall column, *Ind. Eng. Chem. Res.* 52 (2013) 5384–5399, <https://doi.org/10.1021/ie3035898>.
- [10] A. Yang, Y. Su, S. Sun, W. Shen, M. Bai, J. Ren, Towards sustainable separation of the ternary azeotropic mixture based on the intensified reactive-extractive distillation configurations and multi-objective particle swarm optimization, *J. Clean. Prod.* 332 (2022), <https://doi.org/10.1016/j.jclepro.2021.130116>.
- [11] J. Liu, G. Wan, M. Dong, J. Kong, Y. Wu, S. Han, L. Sun, Dynamic controllability strategy of reactive-extractive dividing wall column for the separation of water-containing ternary azeotropic mixture, *Sep. Purif. Technol.* 304 (2023) 122338, <https://doi.org/10.1016/j.seppur.2022.122338>.
- [12] J. Yan, J. Liu, J. Ren, Y. Wu, X. Li, T. Sun, L. Sun, Design and multi-objective optimization of hybrid reactive-extractive distillation process for separating wastewater containing benzene and isopropanol, *Sep. Purif. Technol.* 290 (2022) 120915, <https://doi.org/10.1016/j.seppur.2022.120915>.
- [13] J. Huang, Q. Zhang, C. Liu, T. Yin, W. Xiang, Optimal design of the ternary azeotrope separation process assisted by reactive-extractive distillation for ethyl acetate/isopropanol/water, *Sep. Purif. Technol.* 306 (2023) 122708, <https://doi.org/10.1016/j.seppur.2022.122708>.
- [14] A. Yang, Z.Y. Kong, J. Sunarso, Design and optimisation of novel hybrid side-stream reactive-extractive distillation for recovery of isopropyl alcohol and ethyl acetate from wastewater, *Chem. Eng. J.* 451 (2023) 138563, <https://doi.org/10.1016/j.cej.2022.138563>.
- [15] Y.-Y. Chen, Z.Y. Kong, H.-Y. Lee, A new hybrid reactive-extractive distillation configuration for ternary azeotropic separation with intensification opportunity, *Sep. Purif. Technol.* 335 (2024) 126220, <https://doi.org/10.1016/j.seppur.2023.126220>.
- [16] S. Tututi-Avila, N. Medina-Herrera, J. Hahn, A. Jiménez-Gutiérrez, Design of an energy-efficient side-stream extractive distillation system, *Comput. Chem. Eng.* 102 (2017) 17–25, <https://doi.org/10.1016/j.compchemeng.2016.12.001>.
- [17] Y. Cui, Z. Zhang, X. Shi, C. Guang, J. Gao, Triple-column side-stream extractive distillation optimization via simulated annealing for the benzene/isopropanol/water separation, *Sep. Purif. Technol.* 236 (2020), <https://doi.org/10.1016/j.seppur.2019.116303>.
- [18] C. Cui, Q. Zhang, X. Zhang, J. Sun, Eliminating the vapor split in dividing wall columns through controllable double liquid-only side-stream distillation configuration, *Sep. Purif. Technol.* 242 (2020) 116837, <https://doi.org/10.1016/j.seppur.2020.116837>.
- [19] Z.Y. Kong, J. Sunarso, A. Yang, Recent progress on hybrid reactive-extractive distillation for azeotropic separation: a short review, *Front. Chem. Eng.* 4 (2022).
- [20] Z.Y. Kong, E. Sánchez-Ramírez, A. Yang, W. Shen, J.G. Segovia-Hernández, J. Sunarso, Process intensification from conventional to advanced distillations: past, present, and future, *Chem. Eng. Res. Des.* 188 (2022) 378–392, <https://doi.org/10.1016/j.cherd.2022.09.056>.
- [21] I.A.X. Teh, H.-Y. Lee, Z.Y. Kong, A. Putranto, J. Zheng, J. Sunarso, Unfavorable process intensification of double column reactive extractive distillation system, *Chem. Eng. Process. – Process Intensif.* 196 (2024) 109657, <https://doi.org/10.1016/j.cep.2023.109657>.
- [22] Z.Y. Kong, A. Yang, J.G. Segovia-Hernández, A. Putranto, J. Sunarso, Towards sustainable separation and recovery of dichloromethane and methanol azeotropic mixture through process design, control, and intensification, *J. Chem. Technol. Biotechnol. n/a* (2022), <https://doi.org/10.1002/jctb.7237>.
- [23] Y.C. Wu, H.Y. Lee, H.P. Huang, I.L. Chien, Energy-saving dividing-wall column design and control for heterogeneous azeotropic distillation systems, *Ind. Eng. Chem. Res.* 53 (2014) 1537–1552, <https://doi.org/10.1021/ie403136m>.
- [24] E. Sánchez-Ramírez, S. Sun, J.Y. Sim, A. Yang, Z.Y. Kong, J.G. Segovia-Hernández, A more appropriate way to optimize the hybrid reactive-extractive distillation system, *Sep. Purif. Technol.* 344 (2024) 127184, <https://doi.org/10.1016/j.seppur.2024.127184>.
- [25] A. Yang, Y. Su, S. Sun, W. Shen, M. Bai, J. Ren, Towards sustainable separation of the ternary azeotropic mixture based on the intensified reactive-extractive distillation configurations and multi-objective particle swarm optimization, *J. Clean. Prod.* 332 (2022) 130116, <https://doi.org/10.1016/j.jclepro.2021.130116>.
- [26] M. Srinivas, G.P. Rangaiah, Differential evolution with tabu list for solving nonlinear and mixed-integer nonlinear programming problems, *Ind. Eng. Chem. Res.* 46 (2007) 7126–7135, <https://doi.org/10.1021/ie070007q>.
- [27] A.J. Finn, Rapid assessment of thermally coupled side columns, *Gas Sep. Purif.* 10 (1996) 169–175.

- [28] Z.Y. Kong, J.G. Segovia-Hernández, H.-Y. Lee, J. Sunarso, Are process-intensified extractive distillation always energetically more efficient? *Chem. Eng. Process. – Process Intensif.* 181 (2022) 109131 <https://doi.org/10.1016/j.cep.2022.109131>.
- [29] H. Mo, H. Lee, W. Jang, K. Namgung, J.W. Lee, Unfavorable energy integration of reactive dividing wall column for simultaneous esterification reactions, *Korean J. Chem. Eng.* 38 (2021) 195–203, <https://doi.org/10.1007/s11814-020-0682-3>.
- [30] J.M. Amezcua-Ortiz, H. Alcocer-Garcia, G. Contreras-Zarazua, J. Fontalvo, J. G. Segovia-Hernandez, Sustainable process design for acetone purification produced via dehydrogenation of 2-propanol, *Ind. Eng. Chem. Res.* 61 (2022) 3660–3671, <https://doi.org/10.1021/acs.iecr.1c04321>.